SUPPLEMENTAL MATERIAL

Type-I superconductivity in the Dirac semimetal $PdTe_2$ probed by μSR

H. Leng[1], J.-C. Orain[2], A. Amato[2], Y. K. Huang[1], and A. de Visser[1]

[1]*Van der Waals - Zeeman Institute, University of Amsterdam,*
Science Park 904, 1098 XH Amsterdam, The Netherlands
[2]*Laboratory for Muon-Spin Spectroscopy, Paul Scherrer Institute, 5232 Villigen PSI, Switzerland*

1. Powder X-ray diffraction

A powder X-ray diffraction pattern was measured on a crushed piece of the $PdTe_2$ single crystal, see Fig. S1. The diffraction pattern, taken with Cu-K_α radiation, confirms the CdI_2 crystal structure with lattice parameters $a = 4.034$ Å and $c = 5.132$ Å. The pattern shows single phase homogeneity within the experimental resolution (5 %).

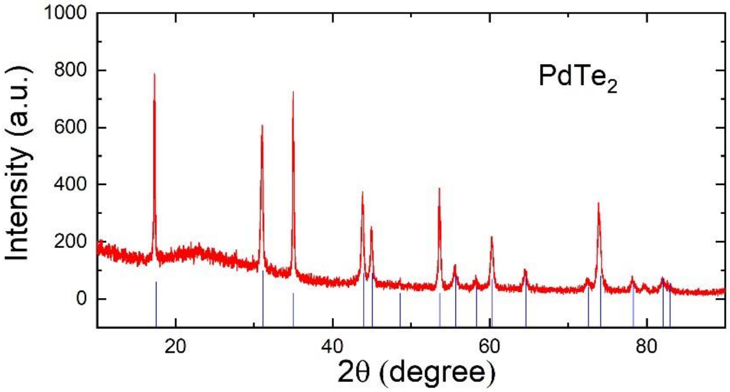

Fig. S1 Powder diffraction pattern of $PdTe_2$. The blue lines indicate the expected Bragg positions.

2. Energy dispersive X-ray spectroscopy

Scanning electron microscopy (SEM; Hitachi TM3000) and energy dispersive X-ray spectroscopy (EDX; Quantax 70) were carried out on the surface of the $PdTe_2$ crystal. A typical EDX spectrum is shown in Fig. S2. Surface scans indicate a homogenous distribution of Pd and Te. EDX spectra measured at several positions on the surface show the expected stoichiometry of 1:2 within the experimental resolution of 0.5 %.

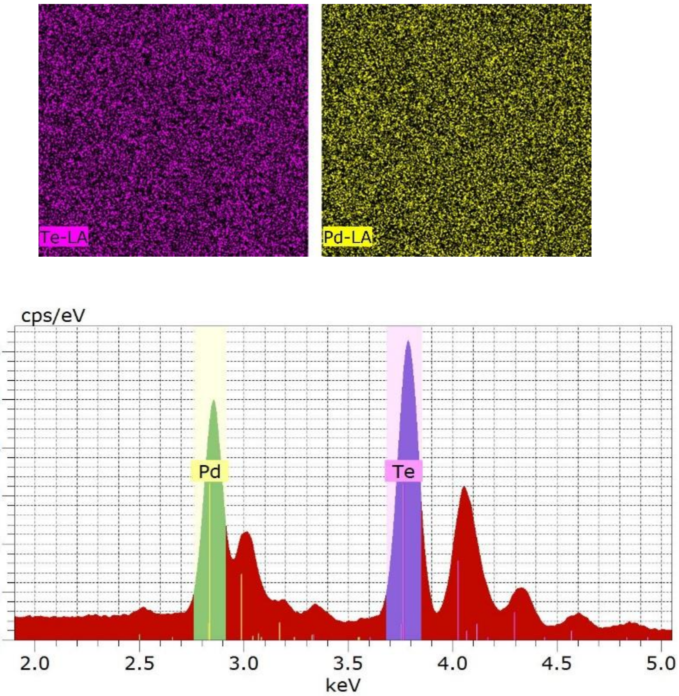

Fig. S2 EDX analysis of the surface of $PdTe_2$. The surface scans (upper panels, scanned area $360\mu m \times 385\ \mu m$.) show the distribution of Pd and Te is homogeneous. The EDX spectrum (lower panel) gives a Pd : Te ratio 33.2 : 66.8.

3. Estimate of the demagnetization factors $N_\perp$ and $N_\|$

The single crystal used for the μSR measurements had a disk-like shape with the *c*-axis perpendicular to the plane of the disk. Its thickness and diameter were 0.65 mm and 10 mm, respectively. A small piece was removed from the disk along the *a*-axis for other measurements. This reduced the size in the perpendicular *a**-direction to 6.8 mm and hampered the precise calculation of *N*. For the configuration with the field applied along the *c*-axis ($N_\perp$) we made two approximations. Assuming the crystal is a short cylinder with diameter 10 mm we calculate $N_\perp$ = 0.88 (Ref. 1). Assuming the crystal is a rectangular bar with size $10\times6.8\times0.65$ mm^3 we calculate $N_\perp$ = 0.86 (Ref. 2). In the manuscript we use the average value $N_\perp = 0.87\pm0.02$, where the error is partly due to the uncertainty in the dimensions of the sample. Under the assumption that $N = N_\perp + 2N_\| = 1$, we calculate for the field in the plane of the disk $N_\| = 0.07$. On the other hand, the calculated value of the radial demagnetization factor of the short cylinder is $N_\| = 0.09$ (Ref. 3). Again, in the manuscript we use the average value $N_\| = 0.08\pm0.02$. We remark these values are obtained for a complete diamagnetic screening, $\chi = -1$.

4. Temperature variation of the μSR damping rate

The field and temperature variations of the different relaxation rates derived from fitting the μSR spectra to Eqs. 1-3 are shown in Fig. S3. In the left diagram $\sigma(H)$ is traced for the configuration with the applied field perpendicular to the plane of the disk and in the right panel $\sigma(T)$ for the field in the plane of the disk. Note the volume fraction of the background contribution is always relatively small, ~ 10%.

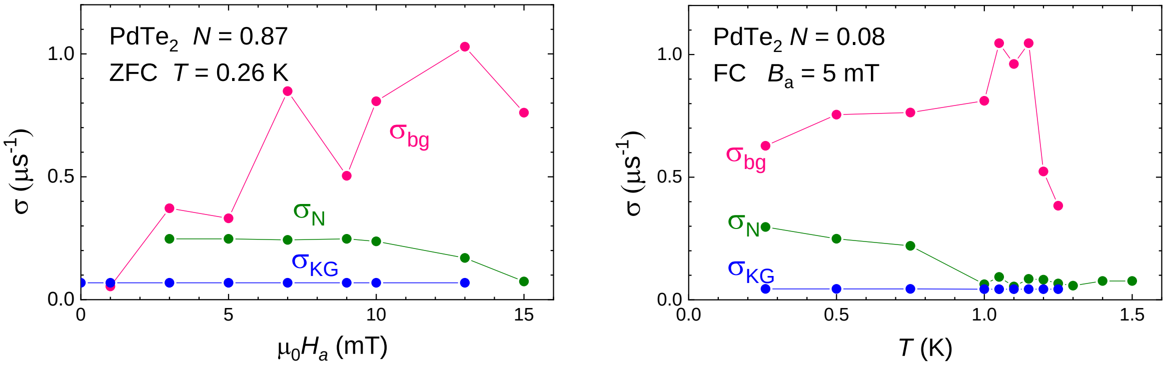

Fig. S3 Field (left panel) and temperature (right panel) variation of the μSR relaxation rate for the Meissner phase, σ_{KG}*, the intermediate or normal phase,* σ_N*, and the background contribution,* σ_{bg}*.*

References

1. D.-X. Chen, J.A. Brug and R.B. Goldfarb, IEEE Trans. Magn. **27**, 3601 (1991).
2. E. Pardo, D.-X. Chen and A. Sanchez, J. Appl. Phys. **96**, 5365 (2004).
3. D.-X. Chen, E. Pardo and A. Sanchez, IEEE Trans. Magn. **37**, 3877 (2001).